Cerebral Cortex, 2022;32: 1260–1268

https://doi.org/10.1093/cercor/bhab291
Advance Access Publication Date: 19 August 2021
Original Article

ORIGINAL ARTICLE

Alpha-Band Phase Modulates Bottom-up Feature Processing

Jianrong Jia[1,2,3,†], Ying Fan[4,5,6,†] and Huan Luo[4,5,6]

[1]Center for Cognition and Brain Disorders of Affiliated Hospital, Hangzhou Normal University, Hangzhou, Zhejiang 310015, China, [2]Institute of Psychological Sciences, Hangzhou Normal University, Hangzhou, Zhejiang 311121, China, [3]Zhejiang Key Laboratory for Research in Assessment of Cognitive Impairments, Hangzhou Normal University, Hangzhou, Zhejiang 311121, China, [4]School of Psychological and Cognitive Sciences, Peking University, Beijing 100871, China, [5]IDG/McGovern Institute for Brain Research, Peking University, Beijing 100871, China and [6]Beijing Key Laboratory of Behavior and Mental Health, Peking University, Beijing 100871, China

Address correspondence to Jianrong Jia, Institute of Psychological Sciences, Hangzhou Normal University, No. 2318 Yuhangtang Road, Yuhang District, 311121 Hangzhou, Zhejiang, China. Email: jianrongjia@hznu.edu.cn and Huan Luo, School of Psychological and Cognitive Sciences, Peking University, No. 5 Yiheyuan Road, Haidian District 100871, Beijing, China. Email: huan.luo@pku.edu.cn

[†]Jianrong Jia and Ying Fan are co-first authors.

Abstract

Recent studies reveal that attention operates in a rhythmic manner, that is, sampling each location or feature alternatively over time. However, most evidence derives from top-down tasks, and it remains elusive whether bottom-up processing also entails dynamic coordination. Here, we developed a novel feature processing paradigm and combined time-resolved behavioral measurements and electroencephalogram (EEG) recordings to address the question. Specifically, a salient color in a multicolor display serves as a noninformative cue to capture attention and presumably reset the oscillations of feature processing. We then measured the behavioral performance of a probe stimulus associated with either high- or low-salient color at varied temporal lags after the cue. First, the behavioral results (i.e., reaction time) display an alpha-band (~8 Hz) profile with a consistent phase lag between high- and low-salient conditions. Second, simultaneous EEG recordings show that behavioral performance is modulated by the phase of alpha-band neural oscillation at the onset of the probes. Finally, high- and low-salient probes are associated with distinct preferred phases of alpha-band neural oscillations. Taken together, our behavioral and neural results convergingly support a central function of alpha-band rhythms in feature processing, that is, features with varied saliency levels are processed at different phases of alpha neural oscillations.

Key words: alpha-band, behavioral oscillation, feature processing, feature-based attention, phase modulation

Introduction

Attention could act on single or multiple items to facilitate information processing. Recent studies demonstrate that, instead of dwelling on multiple items simultaneously, attention tends to operate in a rhythmic manner, that is, processing each location or object alternatively over time (VanRullen 2016; Fiebelkorn and Kastner 2019). In addition to top-down modulation, attention could also occur in a bottom-up way, for example, being automatically captured to a location of high saliency (Gottlieb et al. 1998; Zhang et al. 2012) and forming a saliency map to guide subsequent attentional shifting (Koch and Ullman 1985). An intriguing hypothesis to be tested is whether bottom-up processing in terms of different saliency levels would employ a similar dynamic coordination approach as top-down attentional modulation does to mediate resource allocation.

It has long been known that the phase of neural oscillation serves as a key index for rhythmic processing in the brain

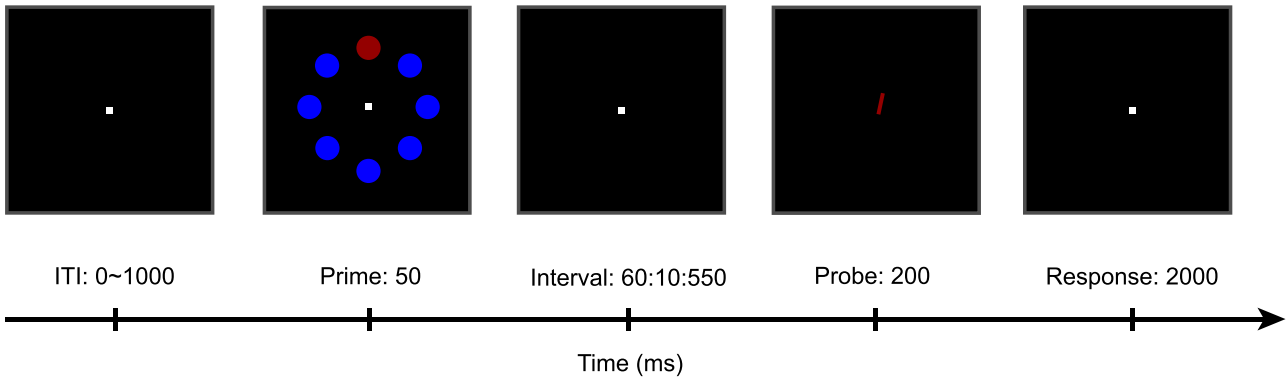

Figure 1. Bottom-up feature processing task. In each trial, a cue display consisting of 8 colored disks (1 in red and 7 in blue, or vice versa) was presented for 50 ms to manipulate the saliency of color features, for example, red is the salient color in this example. After a variable interval (60:10:550 ms, time-resolved behavioral measurements), a probe (i.e., bar stimulus) tilted in either clockwise or anticlockwise direction was presented for 200 ms at the center and subjects made a speedy discrimination on the tilting orientation, regardless of its color. The response duration was fixed at 2000 ms, and next trial started after an additional varied inter-trial interval (ITI) ranging from 0 to 1000 ms. The idea is that the high-salient color (e.g., red here) would presumably capture attention and speed up the detection of probe with high- versus low-salient color. The prime display serves as a noninformative cue to reset the dynamics of feature priming effect, in analogy to the peripheral precue in spatial attentional task. All trials were then classified into high- or low-salient conditions based on whether the probe color was high or low salient in the preceding prime display, for example, the example trial is a high-salient condition.

(Landau et al. 2015; VanRullen 2016; Fiebelkorn et al. 2018; Helfrich et al. 2018). The idea is that if neural oscillations indeed subserve the visual processing by rhythmically modulating the excitability of neural populations that encode particular location or feature, we would expect a phase-dependent profile in the recorded brain signals. Indeed, recent studies have revealed phase-dependent profiles, particularly in spatial attentional tasks (Landau et al. 2015; Helfrich et al. 2018). Meanwhile, since feature-based processing operates across all spatial locations, that is, enhancing the representation of task-related features throughout the whole visual field (Maunsell and Treue 2006; Liu and Hou 2011; Liu 2019), it is not straightforward to directly infer multifeature attention based on previous space- and object-based attention literature.

In the present study, we combined time-resolved behavioral measurements and electroencephalography (EEG) recordings to examine the rhythmic hypothesis of bottom-up feature processing. Specifically, we designed a novel behavioral paradigm motivated by the classical precueing task in space- and object-based attention (Fiebelkorn et al. 2013; Song et al. 2014; Jia et al. 2017), whereby a color singleton (1 high-salient color item in 7 low-salient color items) acts as a noninformative cue in feature space to capture attention and would presumably reset the attentional time course (Fig. 1). As a result, by measuring the behavioral performance of subsequent probe associated with either high-salient or low-salient color features at varied temporal lags after the cue, we could access the fine temporal dynamics of the effect of feature processing (Theeuwes 2013; Theeuwes and Van der Burg 2013; Qian and Liu 2015). The behavioral results showed an alpha-band (~8 Hz) rhythmic profile with a consistent phase lag between high- and low-salient conditions.

Based on the behavioral results, we further examined their relationship to the phase of alpha-band neural oscillations, revealing that the behavioral performance (i.e., RT) was indeed modulated by the alpha-band phase at the onset of the probes, for both high- and low-saliency conditions. Importantly, the 2 conditions showed distinct preferred phase coupled to behavioral performance, that is, better behavioral performance (fastest RT) is coupled to distinct phase of the alpha-band neural oscillations. Taken together, our behavioral and neural recordings convergingly support the crucial function of alpha-band neural oscillations in bottom-up feature processing, that is, features with varied saliency level are sampled at varied phases of alpha rhythms.

Materials and Methods

Subjects

Thirty-one subjects aged 18–27 (15 females) took part in the experiment. All subjects had normal or corrected-to-normal vision and had no history of psychiatric or neurological disorders. The experiment was conducted in accordance with the Declaration of Helsinki. All subjects provided written informed consent, which was approved by the Research Ethics Committee of Peking University, prior to the start of experiment.

Stimuli and Tasks

The experiment was performed in a dark and sound-shielding room, and the visual stimuli were presented on a Display++ LCD monitor (Cambridge Research Systems) with 1920×1080 spatial resolution and 100 Hz refresh rate. Subjects sat at a distance of 70 cm from the monitor, with their heads stabilized on a chin rest. Subjects voluntarily started the experiment by a keypress. In each trial, a visual display (i.e., prime) containing 8 colored disks (radius of 2°) was presented (in 10° visual angle) for 50 ms, and subjects were instructed to maintain central fixation throughout the whole trial (Fig. 1). Specifically, the color of the 8 disks was set to be either 1 in red and 7 in blue or vice versa (1 in blue and 7 in red), and the disk with deviant color was located on either the upper or the lower position to the center. Next, after a varied time interval (stimulus-onset asynchrony (SOA), 60–550 ms in step of 10 ms, 50 SOAs), a colored bar stimulus (i.e., probe, 1.5° length and 0.33° width visual angle) titled in 3° to either clockwise or anti-clockwise direction was presented for 200 ms at the center. Subjects needed to report the tilting direction as soon as possible by pressing the corresponding key (left key for anti-clockwise tilt using left hand, right key for clockwise tilt using right hand) and the reaction time (RT) was

recorded using a response pad (Cedrus Corporation, San Pedro, USA). Crucially, the color of the bar stimulus was either red or blue with equal probability. Note that the color was completely task-irrelevant since subjects were only instructed to report the orientation of the probe stimulus. The deviant color was located in either top or bottom position to avoid left/right spatial priming effect on subsequent behavioral performance of target orientation discrimination. The top or bottom position of the singleton stimulus was orthogonal to the directions of probe tilt (left or right). Subjects were instructed to respond within 2000 ms after the probe, and next trial would start after an additional varied interval ranging from 0 to 1000 ms. The luminance of fixation, disks, and probe were 9.8 cd/m^2 and the luminance of background was 0.14 cd/m^2. Each subject completed 2000 trials in total which took about 2.5 h. A forced break was inserted after every 200 trials.

EEG Data Recording and Preprocessing

EEG signals were recorded simultaneously and continuously using 2 BrainAmp amplifiers and 64-channel BrainCap (Brain-Products). Horizontal and vertical electrooculograms were recorded by 2 electrodes around the right eye. The preprocessing was conducted using the FieldTrip toolbox (Oostenveld et al. 2011). EEG data were first re-referenced to the average value of all channels and then offline band-pass filtered between 1 and 40 Hz using a second-order Butterworth IIR filter. Independent component analysis was then performed to remove eye movement and other artifact components, and the remaining components were back-projected to the electrode space. The EEG signals were next downsampled to 100 Hz. The data were finally segmented into epochs for each trial with 0.65 s before and 0.35 s after the onset of the bar stimulus.

Eye Movement Recording and Analysis

All subjects were instructed to keep the number of eye blinks to a minimum during each trial. Eye movements were continuously monitored using an EyeLink 1000 eye tracker (SR Research). The results showed that the subjects maintained good fixation at the central point (on average across subjects, 98% of eye positions was within 1° of fixation point) throughout all trials.

Analysis of Behavioral Fluctuations

Experimental trials were first classified into 2 conditions (i.e., high-salient, low-salient), based on whether the color of the probe bar stimulus was the high- or low-salient color in the preceding prime display in the current trial. For example, when the prime display contained 7 blue disks and 1 red disk, a bar probe with red color would be assigned to high-salient condition, whereas a bar with blue color would be classified as low-salient condition. Next, for both high- and low-salient conditions, we calculated the RT time course as a function of prime-to-probe SOA (60–550 ms in step of 10 ms, 50 SOAs; median across trials). The behavioral time course was then normalized for each condition and for each subject to remove the individual difference of mean RT across subjects and conditions. The normalized RT time courses were zero-padded to 128 data points in length and then applied by a Hanning window before performing the fast Fourier transform (FFT) analysis. Amplitude and phase spectra were derived by taking the absolute value and the phase value of the complex Fourier coefficients, respectively.

In the frequency domain, oscillations refer to the narrowband peaks of amplitude above the aperiodic component (i.e., 1/f; also known as fractal component) (Buzsáki et al. 2013). Therefore, we parameterized the amplitude spectrum into periodic (i.e., behavioral oscillations) and aperiodic signals using the FOOOF method (Donoghue et al. 2020). Specifically, we first fitted the amplitude spectrum with an aperiodic function defined by a slope and an offset. To obtain a measurement of the periodic signal, we then subtracted this aperiodic function from the original power spectrum, resulting in an aperiodic-adjusted spectrum, which would be regarded as the oscillatory components. The FOOOF toolbox (version 1.0.0) was used to parameterize neural power spectra for each condition (high-salient and low-salient) on each subject, separately (Donoghue et al. 2020). Settings for the algorithm were as follows: peak width limits: (0.5, 12.0); max number of peaks: inf; minimum peak height: 0.0; peak threshold: 2.0; and aperiodic mode: "fixed." Amplitude spectra were parameterized across the frequency range from 2 to 20 Hz.

The subject-wise amplitude spectra were averaged to obtain the group-level results. The phase relationship between high- and low-salient conditions was quantified by the phase differences (high − low) and its distribution uniformity was tested using Rayleigh's test by CircStat Toolbox (Berens 2009).

EEG Modulation of Behavior

In order to test if the ongoing oscillatory activity is related to behavioral performance (i.e., RT here) in each trial, we band-pass filtered the EEG signals into 29 equally spaced bins from 2 to 30 Hz (±center frequency/4) using zero-phase fourth-order Butterworth IIR filter (Fieldtrip toolbox, Oostenveld et al. 2011). All the trials were included into analysis given the high accuracy performance for all subjects. We then applied a Hilbert transform and extracted the instantaneous phase angles and amplitudes. For each EEG channel, we binned the phase angles of each frequency at the probe onset into 36 equally distributed bins and computed the averaged phase-resolved RT across all trials within a 90° window centered on every phase bin. To quantify the nonuniformity of observed RT distribution over phase bins, we calculated the Kullback–Leibler divergence (K–L divergence) of the observed distribution against a uniform mean distribution (Helfrich et al. 2018). To calculate the preferred phase of EEG for each condition, we fitted the RT distribution as a function of phase (ranging from $-\pi$ to π) using a one-term Fourier model (fourier1 in MATLAB). The phase of the peak in the fitted curve was defined as the preferred phase. In addition to phase, we also investigated the effect of amplitude of neural oscillation on behavioral performance by calculating the Pearson correlation between the RT and the amplitude at the probe onset.

Statistical Analysis

The overall accuracy difference between high-salient and low-salient conditions was tested by the paired-sample *t*-test. The overall RT difference between high- and low-salient conditions was tested by the Wilcoxon signed rank test.

Statistical significance of the amplitude spectrum of the RT time course was assessed using permutation tests. In each permutation iteration, we shuffled trials for high- and low-salient conditions separately to generate the surrogate data, in each subject. We then performed FFT analysis and applied the FOOOF algorithm on the surrogate signals to calculate

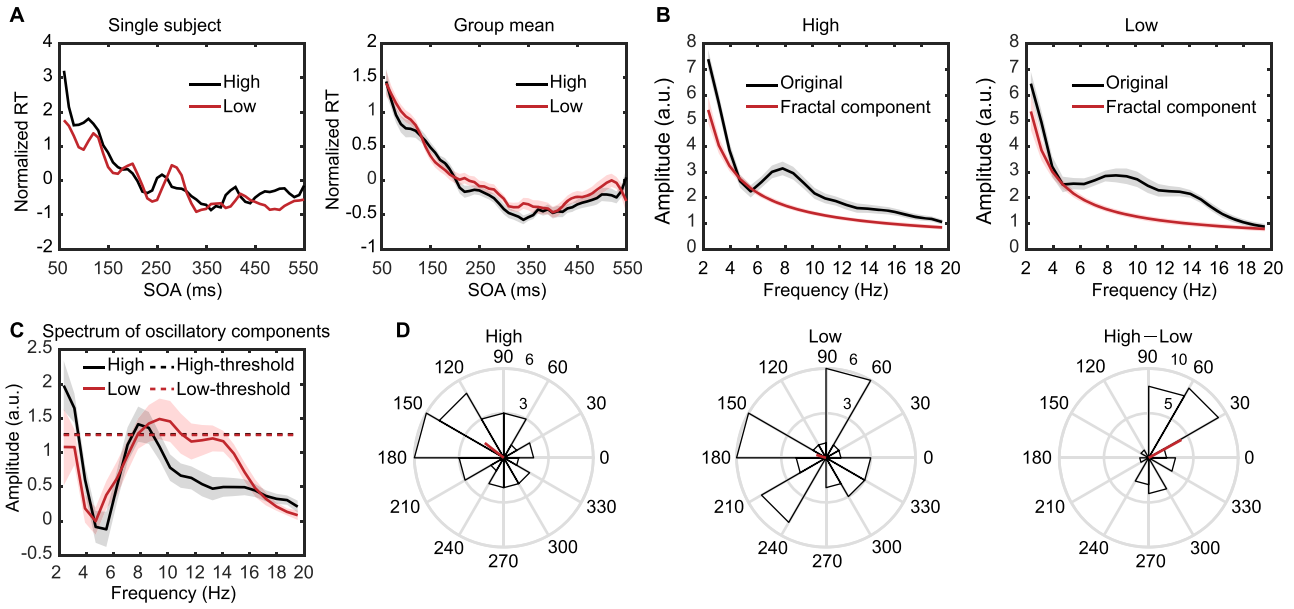

Figure 2. Alpha-band rhythmic profiles in behavioral performance. (*A*) RT time courses (normalized across all SOAs and conditions per subject) as a function of prime-to-probe SOA (60:10:550 ms) for low- (red) and high-salient (black) conditions in a representative subject (left) and grand-averaged results (right). The shaded areas indicate the SEM across subjects ($N = 31$). (*B*) Frequency spectrum (black) and the estimated fractal spectrum component (red) of the RT time course in high- (left) and low-salient (right) conditions. Note that the spectrum analysis was first performed in each subject before being averaged. The shaded areas indicate the SEM across subjects. (*C*) Corrected spectrum (fractal component removed) of the RT time course. The shaded areas indicate the SEM across subjects. Dashed lines indicate the 95% thresholds (permutation test) after multiple comparison correction for high- (black) and low-salient (red) conditions. Note the significant alpha-band (8–10 Hz) peak for both conditions. (*D*) Polar plots of the phase distribution for high-salient (left), low-salient conditions (middle), and their difference (right), across subjects. Note that the significant phase difference clustered around 30° (red line).

the grand-averaged aperiodic-adjusted spectral amplitude. This randomization procedure was repeated 1000 times and yielded a distribution of group-mean spectral amplitude at each frequency bin, from which the threshold ($P = 0.05$, uncorrected) was obtained. To correct for multiple comparison, we used a cross-frequency correction approach (Song et al. 2014), that is, the maximum threshold value across all frequency bins as the threshold. The significant alpha-band frequencies were 7.8–8.6 Hz and 7.8–10.9 Hz for high- and low-salient conditions, respectively (Fig. 2*C*). We next selected their overlapping frequency (i.e., 8 Hz) for further analysis. Statistical assessment of phase difference was conducted using CircStat Toolbox (Berens 2009). For each subject, the phase difference between high- and low-salient conditions at the selected frequency (8 Hz) was computed and then tested using Rayleigh's test for nonuniformity (Zar 2010). The phase difference between the first-half SOAs (i.e., intervals 1–25) and the second-half SOAs (i.e., intervals 26–50) at the peak frequency (8 Hz) was tested using V test for nonuniformity with the mean direction was zero (Zar 2010).

To test the significance of the K–L divergence, we obtained a surrogate distribution by randomly shuffling the trial order of RT in each condition for 1000 times. The shuffling process would disrupt the correspondence between RT and EEG oscillatory phase. The same calculation of K–L divergence was performed on the surrogate data. Through examining the percentile of K–L divergence of observed data in the surrogate distribution, we obtained the statistical significance of EEG-phase modulation on behavior ($P = 1$-percentile) in each EEG channel. The *P* values were FDR-corrected for multiple comparison across channels (Benjamini and Hochberg 1995). In the calculation of K–L divergences for all frequencies, the maximum threshold value across all frequency bins was set as the threshold to correct for multiple comparisons (Song et al. 2014).

The Pearson correlation coefficients between RT and amplitude of 8 Hz neural oscillation were transformed to Fisher's z values first and then tested by one-sample *t*-test for significance and tested by paired-sample *t*-test for difference between conditions.

Results

Alpha-Band Fluctuations in Behavioral Performance

Subjects performed well in the orientation task (Accuracy, mean ± SEM: 0.98 ± 0.003 for high salient, 0.98 ± 0.003 for low salient; no significant difference between the 2 conditions, $t_{(30)} = 0.52$, $P = 0.61$, Cohen's $d = 0.09$, paired-sample *t*-test). Crucially, the overall RT was faster for probe with high-salient color than that with low-salient color (RT, mean ± SEM: 444 ± 12 for high salient, 446 ± 13 for low salient; significant difference between the 2 conditions, $W = 108$, $P = 0.005$, $r_{rb} = -0.56$, Wilcoxon signed rank test), supporting that the feature saliency manipulation in the present design indeed primed attention in a task-irrelevant way.

We next assessed the RT temporal dynamics over SOAs. As shown in Figure 2*A* (left: one representative subject; right: grand average results), in addition to an overall decreasing pattern that is due to expectancy effect (Klein 2000; Song et al. 2014), the normalized RT time courses (converted to *z* scores across all SOAs and all conditions in each subject) showed a rhythmic fluctuation profile for both high- and low-salient conditions. Note that all the subsequent spectrum analyses were performed

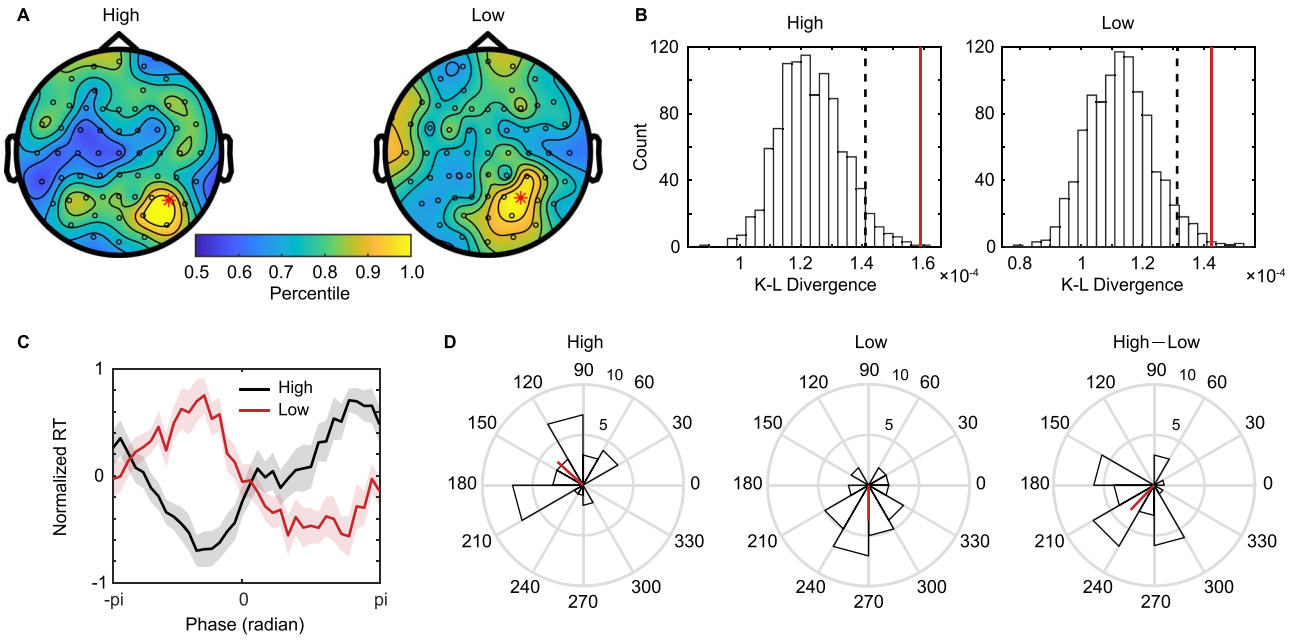

Figure 3. Behavioral performance is modulated by the alpha-band phase in EEG signals. (*A*) Topographic plots of the alpha-band K–L divergence value (percentile in the surrogate distribution from permutation tests) for high- (left) and low-salient (right) conditions. Red stars indicate significant channels (FDR corrected $P < 0.05$, permutation test). (*B*) Surrogate distribution for K–L divergence value for high- (left; P6 channel) and low-salient (right; P4 channel) conditions in the significant channels. The dashed black lines indicate the 95% thresholds in the surrogate distributions and the solid red lines indicate the observed K–L divergence values. (*C*) Behavioral-optimal alpha-band phase, that is, RT as a function of alpha-band phase in EEG signals for high- (black) and low-salient (red) conditions. Noting that the 2 conditions showed distinct optimal phase. (*D*) Polar plots of optimal phases (phase corresponding to the shortest RT) distribution across subjects, for high-salient (left), low-salient (middle) conditions, and their difference (right).

on individual subject before averaging across subject, and therefore, the grand averaged temporal course (Fig. 2A, right) would not necessarily show a clear rhythmic profile given possible loose phase coherence across subjects. We further performed the spectrum analysis on the RT time courses in each subject. First, the nonoscillatory fractal component (1/f component) was estimated (red line in Fig. 2B; FOOOF algorithm, Donoghue et al. 2020) and subtracted from the original spectrum (black line, Fig. 2B). As shown in Figure 2C, both the high- (black) and low-salient (red) conditions showed a significant alpha-band peak (~8 to 10 Hz). We then selected the overlapping significant frequency (i.e., 8 Hz) between the 2 conditions to test the phase relationship between them. The phase distributions were uniform in either high-salient ($P = 0.105$, Rayleigh's test; Fig. 2D left) or low-salient conditions ($P = 0.674$, Rayleigh's test; Fig. 2D middle). The 2 conditions exhibited significant phase difference that was clustered around 30° ($P = 0.001$, Rayleigh's test; Fig. 2D right).

Taken together, the prime display, although completely noninformative, captures attention to the salient feature and presumably resets the oscillations of feature priming effect, leading to the rhythmic profiles of behavioral performance in both high-salient and low salient conditions.

Alpha-Band Neural Phase Underlies Behavioral Fluctuations

After revealing the alpha-band fluctuation in behavioral performance, we next examined its relationship to the concurrently recorded EEG signals. A hypothesis is that the rhythmic performance of high- and low-salient features at behavioral level arises from the underlying periodic fluctuations of neural excitability around the probe's presentation (VanRullen 2016; Fiebelkorn et al. 2018; Helfrich et al. 2018). To test this idea, we calculated the alpha-band phase (8 Hz, the same alpha-band frequency in behavioral performance) of the EEG signals at the onset of the probe stimuli, in each trial and in each EEG channel individually. We then binned the phase angles into 36 equally distributed ranges and calculated the corresponding averaged RTs within each phase bin, for high- and low- salient probes separately. If RT is indeed dependent on the alpha-band phase of EEG signals at the onset of the probe, we would expect a nonuniform RT distribution profile as a function of alpha-band phase. This was quantified by calculating the K–L divergence index (Helfrich et al. 2018). As shown in Figure 3A plotting the topography of K–L divergence results (percentile within the surrogate distribution after permutation tests), the alpha-band phase in the right post-parietal area (red stars) showed significant K–L divergence index for both high- (left) and low-salient (right) conditions (FDR corrected $P < 0.05$, permutation test), supporting the essential relationship between the alpha-band phase in EEG signals and behavioral performance (i.e., RT). Figure 3B illustrates the surrogate distribution for K–L divergence for high- (P6 channel) and low-salient (P4 channel) conditions in the significant channels. The dashed black lines indicate the 95% thresholds in the surrogate distributions and the solid red lines indicate the observed K–L divergence values.

Furthermore, we examined the optimal alpha-band phase (i.e., phase that corresponds to the shortest RT) for high- and low-salient conditions separately. Interestingly, as displayed in Figure 3C, the 2 conditions showed an out-of-phase pattern, such as the optimal phase for low-salient probe (red) was associated with worse performance for high-salient probe (black), whereas the optimal phase for high-salient probe

corresponded to worse performance for low-salient condition. The EEG preferred phases were relatively consistent across subjects for both high- and low-salient conditions (Fig. 3D left and middle, $Ps < 0.001$, Rayleigh's test). The optimal phase difference between high- and low-salient conditions was around 250° (Rayleigh's test for uniformity, $P = 0.019$; Fig. 3D right). Finally, the optimal phase was robust and not different across small and large SOA ranges, for both high- (left; V test, $P < 0.001$) and low-salient (right; V test, $P < 0.001$) conditions (Supplementary Fig. S1).

To examine whether the alpha-band phase calculated around probe onset reflected poststimulus-evoked response, we used a shorter window (from −0.65 to +0.05 s, excluding the effect of poststimulus-evoked responses that presumably occurs after 100 ms, Hillyard and Anllo-Vento 1998). The results confirmed that the alpha-phase modulation was not due to the poststimulus-evoked responses and appeared before and around the probe onset (Supplementary Fig. S2). Furthermore, we compared the poststimulus-evoked responses between high- and low-salient conditions and did not find any difference (supplementary Fig. S3), further confirming that the phase modulations were not affected by poststimulus-evoked responses.

Taken together, the alpha-band behavioral performance is accompanied by the alpha-band phase modulation in EEG signals, supporting the phase–RT modulation relationship. Most interestingly, the high- and low-salient probes tend to be associated with distinct optimal alpha-band phases.

Control Analyses: Other Frequencies and Alpha-Band Power

We only analyzed the alpha-band neural signals (Fig. 3), given the observed behavioral rhythms in the alpha-band (Fig. 2). Meanwhile, it is possible that other neural rhythms are also involved in the process. To address the issue, we calculated the K–L divergence in terms of the relationship between neural phase and behavior in other frequencies. As shown in Figure 4A, only the alpha-band (~8 to 10 Hz) showed significant nonuniform modulation relationship to RTs ($P < 0.05$; Fig. 4B).

Furthermore, previous studies demonstrate that individual variability in alpha neural oscillations can predict individual difference in behavior (e.g., Gulbinaite et al. 2017). Motivated by the findings, we identified the alpha peak frequency (from 7 to 13 Hz) in behavioral performance and that in the EEG recordings in each subject. The 2 alpha-band peak frequencies showed significant correlations across subjects, for both high- and low-salient conditions (Pearson correlation, both $Ps < 0.05$; Supplementary Fig. S4).

Finally, we calculated the correlation between RT and the amplitude of alpha-band neural oscillations. As shown in Figure 4C, alpha-band amplitude showed significant positive correlations to RTs for both high- and low-salient conditions (Fisher's $z = 0.07$, $P < 0.001$ for high-salient; Fisher's $z = 0.06$, $P < 0.001$ for low-salient), and there was no difference between the 2 conditions ($P = 0.31$, paired-sample t-test).

Discussions

We used time-resolved behavioral measurements and concurrent electroencephalogram (EEG) recordings to examine the temporal dynamics of bottom-up feature processing. First, after an uninformative cue that attracts attention to a salient feature, the behavioral performance of the subsequent high- and low-salient probes displays an alpha-band rhythmic profile with a consistent phase lag. Second, behavioral performance is further modulated by the alpha-band phase in the EEG recordings around the probe. Third, high- and low-salient conditions show varied optimal alpha-band phases, that is, high- and low-salient features tend to be processed in distinct phases of alpha-band neural oscillations. Taken together, the present study provides converging behavioral and neural evidence speaking to a central role of alpha-band neural oscillation in feature processing, that is, features with varied saliency levels are processed at different phases of alpha neural oscillations.

Although top-down attention has been widely studied, how bottom-up processing operates in a multi-item context remains less explored (noting that bottom-up feature attention is still controversial and varies in different experiment paradigms, for example, Donovan et al. 2020). In the present study, subject performed an orientation discrimination task and the color feature was completely task-irrelevant and noninformative but was still found to be processed automatically via alpha-band rhythm. Jensen et al. (2012) proposed an oscillation-based model for the neural representations of unattended items, that is, alpha-band neural oscillations prioritize and sort unattended visual inputs in time according to their saliency levels. Specifically, since alpha-band exerts an inhibitory function, when alpha-band power gradually decreases, the unattended stimuli would be disinhibited and in turn activate sequentially based on their respective excitation levels, leading to an alpha-band phase code for unattended items (Jensen et al. 2012; Jia et al. 2019). In the present study, the salient but task-irrelevant color feature automatically attracts attention and in turn recovers from the alpha-band inhibition earlier compared to low-salient feature, leading to an ongoing competition between high- and low-salient features in the alpha-band rhythm. The observed distinct optimal phases for high- and low-salient features are also consistent with the model prediction, that is, features with different saliency levels are recovered from inhibition at different phases within an alpha-band cycle.

The present study is motivated by previous precueing spatial attention studies (Landau and Fries 2012; Fiebelkorn et al. 2013; Song et al. 2014), that is, using uninformative cue to capture attention to one location and examining following probes at cued or uncued locations. Here, the singleton in multicolor display serves as an uninformative cue in feature space, capturing attention to specific color. The following probe associated with either high- or low-salient color could thus be used to test feature attentional capture effects, in analogy to cued or uncued location in spatial task. Meanwhile, different from precueing spatial paradigm during which both cued and uncued locations are present, there is only 1 single-colored probe, which does not seemingly necessitate a feature-based attentional selection process. Instead, our paradigm might be more related to feature priming paradigm (Kristjánsson and Campana 2010; Theeuwes 2013) and previous studies have also revealed rhythmic fluctuations in priming behavioral performance (Huang et al. 2015; Wang et al. 2020). In other words, the salient color in multicolor display serves as a prime in feature space and influences subsequent probe performance.

Our results are consistent with previous findings demonstrating the crucial relationship between oscillatory phase and visual perception (Busch et al. 2009; Dugue et al. 2011; Chakravarthi and VanRullen 2012; Ronconi and Melcher 2017), that is, near-threshold visual perception is dependent on the

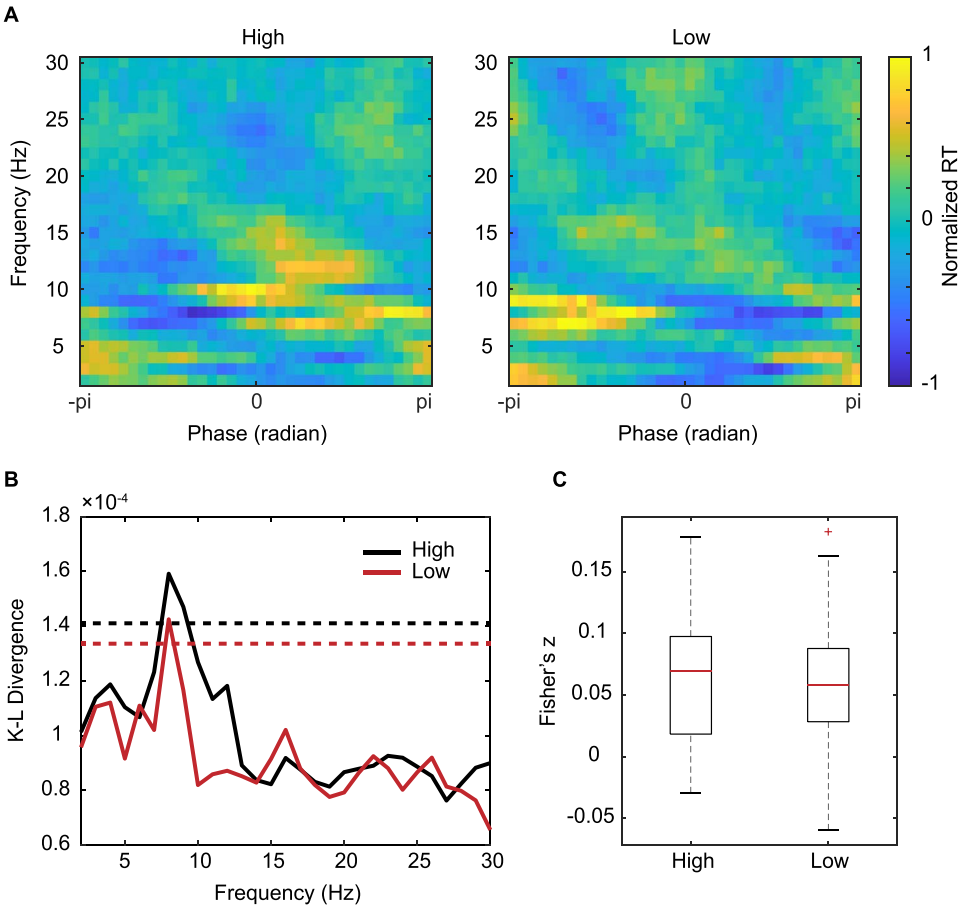

Figure 4. Other frequencies and alpha-band power. (A) RT as a function of phase (x-axis) and frequency (y-axis) for both high- (left) and low-salient (right) conditions. Note that the phase modulation of RT is specific to alpha-band (~8 to 10 Hz). (B) K–L divergence value (phase-RT) as a function of frequencies. Dashed lines: Corrected threshold after multi-comparison, for high- (black) and low-salient (red) conditions. (C) Correlations between RT and alpha-band amplitude for high- and low-salient conditions. Note that the correlation coefficients were transformed to Fisher's z values.

prestimulus phase of theta- and alpha-band neural oscillations. Moreover, a recent study by Harris et al. (2018) revealed that detection of both attended and unattended stimuli relies on the theta- and alpha-band phases of neural oscillations, supporting a general role of low-frequency neural rhythms in mediating attentional resource allocation. Furthermore, we demonstrate that the alpha-band power is positively correlated with the RT for both high- and low-salient conditions. This is also in line with the well-known inhibitory role of alpha-band neural oscillation (Klimesch 2012; Jensen et al. 2014), such as that the stronger alpha-band power is associated with lower excitability of neural network and accordingly worse behavioral performance (Jensen et al. 2012; Klimesch 2012; Hutchinson et al. 2021). Thus, both power and phase of alpha-band rhythms contribute to visual attention, whereby the power reflects general inhibitory level, and the phase flexibly determines resource organization among items over time.

Is there any single rhythm for all types of visual perception and attention? Previous evidence would not support the view and instead posits that brain oscillations at various rhythms might work together to mediate information coordination in the brain (Ronconi et al. 2017). For example, single-item perception has been found to be more linked to alpha-band rhythm (VanRullen et al. 2007; Fiebelkorn et al. 2013; Re et al. 2019), whereas multi-item attention is proposed to entail theta-band rhythm (Landau and Fries 2012; Song et al. 2014). One way to reconcile the distinct findings is that alpha-band might serve as the most basic temporal unit for perception, and when multiple locations or objects are processed, the overall attentional sampling frequency would decrease and is determined by the number of items to be processed, leading to the theta-band findings (Fiebelkorn et al. 2013; Fiebelkorn and Kastner 2019; Re et al. 2019). Alternatively, theta-band has been posited to originate from motion exploration such as saccade and serve as an independent role in attentional operation by rhythmically disengaging attention from the current focus-of-attention to support environment exploration (Bosman et al. 2009; Schroeder et al. 2010). Recent studies reveal a theta-band rhythmic coupling between visual perception and movements (Tomassini et al. 2015; Wutz et al. 2016; Benedetto and Morrone 2019), advocating a generally close link between perception and active movement. Our previous works have revealed cross-frequency coupling in both behavioral performance and MEG and EEG recordings. For instance, each location or object is processed via alpha-band, and the alpha-band profiles for multiple items are further coordinated by a theta-band rhythm (Song et al. 2014; Jia et al. 2017). Interestingly, in a top-down feature attention task, both behavioral and neural evidence only disclose a theta-band

rhythmic pattern (Mo et al. 2019; Re et al. 2019). Taken together, neural rhythms at various rhythms are involved in different processes, based on task context and to-be-processed properties (Wutz et al. 2018).

In addition to the alpha-band oscillation, the low-frequency oscillations (~2 Hz), that is, delta-band, have been found to reflect rhythmic shifting of neuronal ensembles between high and low excitability states (Lakatos et al. 2008; Schroeder and Lakatos 2009). Meanwhile, different from the alpha-band rhythm, here the low-frequency components in RT were not modulated by EEG phase. This is consistent with previous findings (VanRullen 2016), revealing that the phase modulation mainly occurs in theta (~7 Hz) and alpha band (~11 Hz). Furthermore, although both behavioral and neural findings show alpha-band fluctuations, they are not within the exactly same frequency, that is, lower and more centered for neural data (Figs 2C and 4B). Interestingly, despite their difference, the 2 alpha-band frequencies exhibited significant correlation across subjects (Supplementary Fig. S4), still supporting their common origin.

The phase lag between high- and low-salient conditions centered around 30° in behavioral measurements but 250° in neural recordings. The behavioral–neural discrepancy might arise from other cognitive processes that contribute to final behavioral performance, such as motor response, decision making, etc. The individual variability results (Fig. 2D) further support the notion, that is, inconsistent phase distribution across subjects and broad alpha-band peak frequency distribution in behavioral measurements. Future studies are needed to systematically test the relationship between behavioral and neural rhythms.

Rhythmic processing is involved in many aspects of perception and attention (Jensen et al. 2012; Fiebelkorn and Kastner 2019) across different sensory modalities, including vision (Drewes et al. 2015), audition (Ho et al. 2017), and sensory-motor integration (Benedetto et al. 2016; Wutz et al. 2016; Benedetto and Morrone 2019). At low levels, attention periodically samples competing stimuli during binocular rivalry (Davidson et al. 2018), and at high levels, multiple predictions are coordinated by an oscillation-based temporal organization process (Huang et al. 2015; Guo et al. 2020; Wang et al. 2020). Our results constitute new evidence that bottom-up feature processing is coordinated by neural oscillations as well. Notably, feature attention in previous research shows a slower rhythmic profile (Mo et al. 2019; Re et al. 2019) when subjects attend to 2 features concurrently, while here in a bottom-up task-irrelevant context, we mainly observed an alpha-band pattern. Therefore, different from top-down modulations, bottom-up feature processing might rely on the opportunity windows that are bound to varied phases of alpha-band rhythms to mediate the processing of unattended features.

In conclusion, the present study, by combining behavioral and neural recordings, demonstrates that bottom-up processing samples multiple features in alpha-band rhythms and items with different saliency levels are processed at varied phases.

Supplementary Material

Supplementary material can be found at *Cerebral Cortex* online.

Funding

National Natural Science Foundation of China (32000735 to J.J., 31930052 to H.L.); Hangzhou Normal University's provincial predominant characteristic discipline cultivation program (19JYXK028) to J.J.; Beijing Municipal Science & Technology Commission (Z181100001518002 to H.L.).

Notes

Conflict of Interest: None declared.

References

Benedetto A, Morrone MC. 2019. Visual sensitivity and bias oscillate phase-locked to saccadic eye movements. *J Vis*. 19:15.

Benedetto A, Spinelli D, Morrone MC. 2016. Rhythmic modulation of visual contrast discrimination triggered by action. *Proc R Soc B Biol Sci*. 283:20160692.

Benjamini Y, Hochberg Y. 1995. Controlling the false discovery rate: a practical and powerful approach to multiple testing. *J R Stat Soc Ser B Methodol*. 57:289–300.

Berens P. 2009. CircStat: a MATLAB toolbox for circular statistics. *J Stat Softw*. 1:1–21.

Bosman CA, Womelsdorf T, Desimone R, Fries P. 2009. A microsaccadic rhythm modulates gamma-band synchronization and behavior. *J Neurosci*. 29:9471–9480.

Busch NA, Dubois J, VanRullen R. 2009. The phase of ongoing EEG oscillations predicts visual perception. *J Neurosci*. 29:7869–7876.

Buzsáki G, Logothetis N, Singer W. 2013. Scaling brain size, keeping timing: evolutionary preservation of brain rhythms. *Neuron*. 80:751–764.

Chakravarthi R, VanRullen R. 2012. Conscious updating is a rhythmic process. *Proc Natl Acad Sci*. 109:10599–10604.

Davidson MJ, Alais D, van Boxtel JJ, Tsuchiya N. 2018. Attention periodically samples competing stimuli during binocular rivalry. *Elife*. 7:e40868.

Donoghue T, Haller M, Peterson EJ, Varma P, Sebastian P, Gao R, Noto T, Lara AH, Wallis JD, Knight RT, et al. 2020. Parameterizing neural power spectra into periodic and aperiodic components. *Nat Neurosci*. 23:1655–1665.

Donovan I, Zhou YJ, Carrasco M. 2020. In search of exogenous feature-based attention. *Atten Percept Psychophys*. 82:312–329.

Drewes J, Zhu W, Wutz A, Melcher D. 2015. Dense sampling reveals behavioral oscillations in rapid visual categorization. *Sci Rep*. 5:16290.

Dugue L, Marque P, VanRullen R. 2011. The phase of ongoing oscillations mediates the causal relation between brain excitation and visual perception. *J Neurosci*. 31:11889–11893.

Fiebelkorn IC, Kastner S. 2019. A rhythmic theory of attention. *Trends Cogn Sci*. 23:87–101.

Fiebelkorn IC, Pinsk MA, Kastner S. 2018. A dynamic interplay within the frontoparietal network underlies rhythmic spatial attention. *Neuron*. 99:842–853.e8.

Fiebelkorn IC, Saalmann YB, Kastner S. 2013. Rhythmic sampling within and between objects despite sustained attention at a cued location. *Curr Biol*. 23:2553–2558.

Gottlieb JP, Kusunoki M, Goldberg ME. 1998. The representation of visual salience in monkey parietal cortex. *Nature*. 391:481–484.

Gulbinaite R, van Viegen T, Wieling M, Cohen MX, VanRullen R. 2017. Individual alpha peak frequency predicts 10 Hz flicker effects on selective attention. *J Neurosci*. 37:10173–10184.

Guo B, Lu Z, Goold JE, Luo H, Meng M. 2020. Fluctuations of fMRI activation patterns in visual object priming. *Hum Behav Brain*. 1:78–84.

Harris AM, Dux PE, Mattingley JB. 2018. Detecting unattended stimuli depends on the phase of prestimulus neural oscillations. *J Neurosci*. 38:3092–3101.

Helfrich RF, Fiebelkorn IC, Szczepanski SM, Lin JJ, Parvizi J, Knight RT, Kastner S. 2018. Neural mechanisms of sustained attention are rhythmic. *Neuron*. 99:854–865.e5.

Hillyard SA, Anllo-Vento L. 1998. Event-related brain potentials in the study of visual selective attention. *Proc Natl Acad Sci*. 95:781–787.

Ho HT, Leung J, Burr DC, Alais D, Morrone MC. 2017. Auditory sensitivity and decision criteria oscillate at different frequencies separately for the two ears. *Curr Biol*. 27:3643–3649.e3.

Huang Y, Chen L, Luo H. 2015. Behavioral oscillation in priming: competing perceptual predictions conveyed in alternating theta-band rhythms. *J Neurosci*. 35:2830–2837.

Hutchinson BT, Pammer K, Jack B. 2021. Pre-stimulus alpha predicts inattentional blindness. *Conscious Cogn*. 87:103034.

Jensen O, Bonnefond M, VanRullen R. 2012. An oscillatory mechanism for prioritizing salient unattended stimuli. *Trends Cogn Sci*. 16:200–206.

Jensen O, Gips B, Bergmann TO, Bonnefond M. 2014. Temporal coding organized by coupled alpha and gamma oscillations prioritize visual processing. *Trends Neurosci*. 37:357–369.

Jia J, Fang F, Luo H. 2019. Selective spatial attention involves two alpha-band components associated with distinct spatiotemporal and functional characteristics. *Neuroimage*. 199: 228–236.

Jia J, Liu L, Fang F, Luo H. 2017. Sequential sampling of visual objects during sustained attention. *PLoS Biol*. 15:e2001903.

Klein RM. 2000. Inhibition of return. *Trends Cogn Sci*. 4:138–147.

Klimesch W. 2012. Alpha-band oscillations, attention, and controlled access to stored information. *Trends Cogn Sci*. 16:606–617.

Koch C, Ullman S. 1985. Shifts in selective visual attention: towards the underlying neural circuitry. *Hum Neurobiol*. 4:219–227.

Kristjánsson Á, Campana G. 2010. Where perception meets memory: a review of repetition priming in visual search tasks. *Atten Percept Psychophys*. 72:5–18.

Lakatos P, Karmos G, Mehta AD, Ulbert I, Schroeder CE. 2008. Entrainment of neuronal oscillations as a mechanism of attentional selection. *Science*. 320:110–113.

Landau AN, Fries P. 2012. Attention samples stimuli rhythmically. *Curr Biol*. 22:1000–1004.

Landau AN, Schreyer HM, van Pelt S, Fries P. 2015. Distributed attention is implemented through theta-rhythmic gamma modulation. *Curr Biol*. 25:2332–2337.

Liu T. 2019. Feature-based attention: effects and control. *Curr Opin Psychol*. 29:187–192.

Liu T, Hou Y. 2011. Global feature-based attention to orientation. *J Vis*. 11:8–8.

Maunsell JH, Treue S. 2006. Feature-based attention in visual cortex. *Trends Neurosci*. 29:317–322.

Mo C, Lu J, Wu B, Jia J, Luo H, Fang F. 2019. Competing rhythmic neural representations of orientations during concurrent attention to multiple orientation features. *Nat Commun*. 10:5264.

Oostenveld R, Fries P, Maris E, Schoffelen J-M. 2011. FieldTrip: open source software for advanced analysis of MEG, EEG, and invasive electrophysiological data. *Comput Intell Neurosci*. 2011:1–9.

Qian C, Liu T. 2015. Involuntary attention in the absence of visual awareness. *Vis Cogn*. 23:840–843.

Re D, Inbar M, Richter CG, Landau AN. 2019. Feature-based attention samples stimuli rhythmically. *Curr Biol*. 29:693–699.e4.

Ronconi L, Melcher D. 2017. The role of oscillatory phase in determining the temporal organization of perception: evidence from sensory entrainment. *J Neurosci*. 37:10636–10644.

Ronconi L, Oosterhof NN, Bonmassar C, Melcher D. 2017. Multiple oscillatory rhythms determine the temporal organization of perception. *Proc Natl Acad Sci*. 114:13435–13440.

Schroeder CE, Lakatos P. 2009. Low-frequency neuronal oscillations as instruments of sensory selection. *Trends Neurosci*. 32:9–18.

Schroeder CE, Wilson DA, Radman T, Scharfman H, Lakatos P. 2010. Dynamics of active sensing and perceptual selection. *Curr Opin Neurobiol*. 20:172–176.

Song K, Meng M, Chen L, Zhou K, Luo H. 2014. Behavioral oscillations in attention: rhythmic α pulses mediated through θ band. *J Neurosci*. 34:4837–4844.

Theeuwes J. 2013. Feature-based attention: it is all bottom-up priming. *Philos Trans R Soc B Biol Sci*. 368:20130055.

Theeuwes J, Van der Burg E. 2013. Priming makes a stimulus more salient. *J Vis*. 13:21–21.

Tomassini A, Spinelli D, Jacono M, Sandini G, Morrone MC. 2015. Rhythmic oscillations of visual contrast sensitivity synchronized with action. *J Neurosci*. 35:7019–7029.

VanRullen R. 2016. Perceptual cycles. *Trends Cogn Sci*. 20: 723–735.

VanRullen R, Carlson T, Cavanagh P. 2007. The blinking spotlight of attention. *Proc Natl Acad Sci*. 104:19204–19209.

Wang M, Huang Y, Luo H, Zhang H. 2020. Sustained visual priming effects can emerge from attentional oscillation and temporal expectation. *J Neurosci*. 40:3657–3674.

Wutz A, Melcher D, Samaha J. 2018. Frequency modulation of neural oscillations according to visual task demands. *Proc Natl Acad Sci*. 115:1346–1351.

Wutz A, Muschter E, van Koningsbruggen MG, Weisz N, Melcher D. 2016. Temporal integration windows in neural processing and perception aligned to saccadic eye movements. *Curr Biol*. 26:1659–1668.

Zar JH. 2010. *Biostatistical analysis*. 5th ed. Upper Saddle River, New Jersey: Pearson Prentice Hall.

Zhang X, Zhaoping L, Zhou T, Fang F. 2012. Neural activities in v1 create a bottom-up saliency map. *Neuron*. 73: 183–192.